Computers and Electronics in Agriculture 80 (2012) 1–7

Contents lists available at SciVerse ScienceDirect

Computers and Electronics in Agriculture

journal homepage: www.elsevier.com/locate/compag

Model fusion for prediction of apple firmness using hyperspectral scattering image

Shuang Wang, Min Huang *, Qibing Zhu

Key Laboratory of Advanced Process Control for Light Industry (Ministry of Education), Jiangnan University, Wuxi 214122, PR China

ARTICLE INFO

Article history:
Received 11 May 2011
Received in revised form 12 October 2011
Accepted 16 October 2011

Keywords:
Hyperspectral scattering image
Wavelength selection
Partial least squares
Uninformative variable elimination
Supervised affinity propagations
Model fusion

ABSTRACT

Hyperspectral scattering image is an advanced technology widely used in non-destructive measurement of fruit quality. To develop a better prediction model for apple firmness, the present study investigates a model fusion method coupled with wavelength selection algorithms. The current paper first discusses two wavelength selection algorithms, namely, uninformative variable elimination (UVE) and supervised affinity propagation (SAP). The selected effective wavelengths are then set as input to the partial least square (PLS) model. Six hundred "Golden Delicious" apples were analyzed. The first 450 apples were used as sample for the calibration model, whereas the remaining 150 were used for the prediction model. Compared with full wavelengths, the number of effective wavelengths based on the UVE and SAP algorithms decreased to 34% and 35%, but the correlation coefficient of prediction (*R*p) increased from 0.791 to 0.805 and 0.814, whereas the root mean-square error of prediction (RMSEP) decreased from 6.00 to 5.73 and 5.71 N, respectively. A fusion model was then developed using UVE-PLS and SAP-PLS models coupled with backpropagation neural network. A better prediction accuracy was achieved from the fusion model (*R*p = 0.828 and RMSEP = 5.53 N). The model fusion provides an effective modeling method for apple firmness prediction using hyperspectral scattering image technique.

1. Introduction

As the living standard of people improves, testing of fruit quality has been increasingly desired, meant not only for external but also for internal qualities, including firmness, soluble solid content (SSC), acid, and juice. An emerging research trend in testing the fruits' internal quality is the shift from using traditional destructive techniques into non-destructive approaches. Many technologies have been studied in this emerging field, including optical, physical, and radiographic technologies (Armstrong et al., 1997; Zude et al., 2006), and so on. Near-infrared (NIR) spectroscopy has played an important role in predicting the internal quality of apples and other fruits (Nicolai et al., 2007; Lu, 2001; Peng and Lu, 2006). However, the results of these studies in predicting fruit firmness were unsatisfactory. For the "Golden Delicious" apples, the correlation coefficient (*R*p) was 0.50, and the root mean-square error of prediction (RMSEP) was 8.64 N (Peng and Lu, 2006). Further studies on rapid and accurate non-destructive measurement of fruit firmness, SSC, and other quality attributes are therefore necessary.

Light scattering occurs when a light beam irradiates a fruit. Part of the light will be absorbed and other parts will scatter in certain patterns. The spectrum of light scattering can give useful information on the structural/physical characteristics of a sample. Using light scattering may yield better prediction of fruit firmness and other quality attributes. In recent years, hyperspectral scattering technology has been used in numerous studies as a non-destructive approach to determine fruit quality attributes. Lu and Peng (2006) described the light scattering technique and investigated hyperspectral scattering as a means to measure firmness of peaches. Peng and Lu (2008) compared different mathematical models for describing hyperspectral scattering profiles to select an optimal model for predicting the firmness and SSC of "Golden Delicious" apples. These studies were able to present new methods for analyzing the spectral scattering images. However, the prediction results of fruit firmness or SSC must be improved because the hyperspectral scattering images contain much redundant information in hundreds of spectral wavelengths. To develop better prediction models of apple firmness, the model fusion method coupled with wavelength selection algorithms is investigated in the present paper. Wavelength selection algorithms have been studied, including correlation coefficient method (Min and Lee, 2005), regression coefficient (Wu et al., 2008), and genetic algorithm (Koumonsis and Katsaras, 2006). Uninformative variable elimination (UVE) (Centner, 2009) is an algorithm for wavelength selection based on analysis of the partial least square (PLS) regression coefficients. UVE is used to evaluate the reliability of every variable in a model using a variable selection criterion and to eliminate uninformative variables. The UVE algorithm has been widely applied in wavelength selection of NIR spectroscopy, achieving good prediction results. The affinity propagation (AP) algorithm (Frey and Dueck, 2007; Qian et al., 2009) uses a similarity matrix from the spectral

* Corresponding author. Address: School of Internet of Things, Jiangnan University, 1800 Lihu Avenue, Wuxi 214122, Jiangsu Province, PR China. Tel.: +86 510 85910635; fax: +86 510 85910633.
E-mail address: huangmzqb@163.com (M. Huang).

0168-1699/$ - see front matter © 2011 Elsevier B.V. All rights reserved.
doi:10.1016/j.compag.2011.10.008

matrix. Unlike other clustering algorithms, AP considers all data points (one wavelength is a data point) as potential cluster centers (exemplars) and then exchanges messages among the data points until a good set of clusters emerges. AP has been applied to computer vision and bioinformatics. Supervised AP (SAP) is a modification of AP. The present study adopted SAP, which used absolute errors between actual firmness and predicted values from each wavelength to adjust the similarity matrix. The selected optimal wavelengths were used to develop prediction models for apple firmness using PLS regression. Previous studies mostly utilized a single algorithm to select the optimal wavelengths. However, the unselected wavelengths may contain useful information that might improve the prediction accuracy of the model. To reduce the limitations of a single algorithm, a model fusion approach is proposed using the backpropagation (BP) artificial neural network to process the data obtained from the UVE-PLS and SAP-PLS prediction models.

The overall objective of the current study is to use the UVE and SAP algorithms for wavelength selection. The BP neural network is utilized to process the data obtained from the two algorithms. The specific steps of the present work are as follows:

- To acquire the hyperspectral scattering images of the "Golden Delicious" apples using a hyperspectral imaging system in the spectral region from 500 to 1000 nm.
- To select the optimal wavelengths using UVE and SAP and develop the prediction model of apple firmness using selected optimal wavelengths coupled with the PLS algorithm.
- To fuse the data obtained from UVE-PLS and SAP-PLS to obtain the best results for apple firmness prediction.

2. Materials and methods

2.1. Apple sample

In the experiment, 600 "Golden Delicious" apples were harvested in 2006 from orchards at Michigan State University (MSU) Clarksville Horticultural Experiment Station in Clarksville and at MSU Horticultural Teaching and Research Center in Holt. Before the experiment, the apples were stored in a controlled atmospheric environment (2% O_2 and 3% CO_2 at 0 °C) for about 5 months. After the apples were kept at room temperature (24 °C) for more than 15 h, the experiment began. The average fruit diameter ranged from 67.50 to 82.78 mm.

2.2. Acquisition of hyperspectral scattering images and spectral profile extraction

A laboratory hyperspectral imaging system was used to acquire the scattering images of the apples. The system is composed of three parts: a high-performance back-illuminated CCD camera (Model C4880-21-24A, Hamamatsu Photonics, Systems, Bridgewater, NJ, USA); an imaging spectrograph (ImSpector V10, Spectral Imaging Ltd., Oulu, Finland) with a spectral range between 400 and 1000 nm; and a quartz tungsten halogen lamp as light source. The nominal spectral resolution for the hyperspectral imaging system was 4.54 nm, and the spatial resolution was 0.20 mm/pixel. The hyperspectral imaging system was spectrally and spatially calibrated using the procedures described by Qin and Lu (2007). Each apple's hyperspectral images were obtained by line scanning an area located 9 mm from its equator. Ten scanned images were obtained at a time and were averaged for data analysis. To correct the light source variation effect, reference scattering images were taken from a white Teflon disk for every 10 apples.

A typical raw hyperspectral scattering image is shown in Fig. 1. The horizontal axis represents the spatial dimension, and the vertical axis shows the spectral dimension. The wavelengths of interest were taken at every 5 nm interval ranging from 500 to 1000 nm. Each sample thus contained 101 wavelengths, and a total spatial distance of 20 mm was selected from each image. The spatial scattering profiles for the apples are shown in Fig. 2 at 650, 750, and 850 nm. The three profiles indicate that the fruit's optical properties are wavelength dependent. The scattering information of the specific wavelengths can fully reflect the physical structure related to the firmness of each fruit. This information was useful in wavelength selection. Each scattering profile was corrected for non-uniform instrument response and fruit size using the method proposed by Qin and Lu (2008).

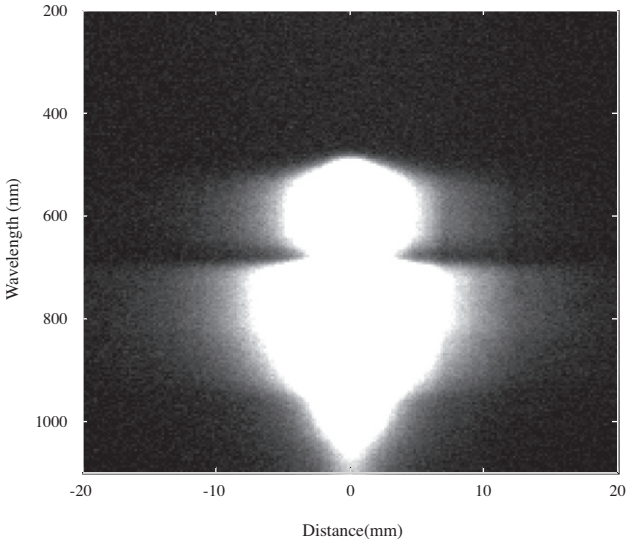

Fig. 1. Typical hyperspectral image for "Golden Delicious" apples.

Different approaches have been used to analyze the hyperspectral scattering images. Spatial scattering profiles at different wavelengths were described by a modified Lorentzian distribution function with four parameters (Peng and Lu, 2006), a diffusion theory model with two parameters (Qin and Lu, 2008), and a mean reflectance model with one parameter (Lu, 2007). In the present study, the simple mean reflectance model was used because it provides good characterization of light scattering features by calculating the mean value of each scattering profile for a specific distance. Mean reflectance $\overline{R}_s$ was obtained by calculating the

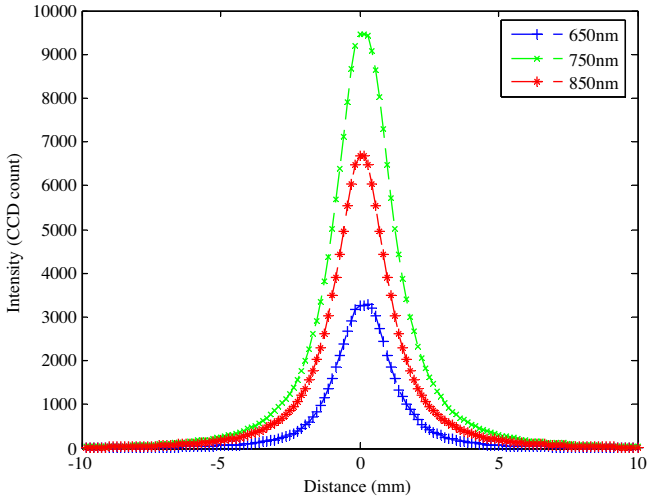

Fig. 2. Raw spatial scattering profiles at three wavelengths.

average reflectance value over the spatial distance of 10 mm for each wavelength of the apples. $\overline{R}_s$ was then corrected by the mean reflectance $\overline{R}_T$ obtained from the white Teflon disk using the equation

$$\overline{R} = \frac{\overline{R}_s}{\overline{R}_T} \text{ for } 0 \le x \le 10 \text{ mm}. \quad (1)$$

2.3. Destructive instrument tests

After the imaging, an 11.0 mm-diameter Magness–Taylor (MT) firmness probe attached to a texture analyzer (TA.XT2i, Stable Micro Systems, Goldalming Surrey, UK) was used to measure the firmness of each apple from the same imaged area. The MT probe penetrated 9 mm deep into the peeled portion of the fruit at a speed of 2 mm/s. The maximum force recorded from the force/displacement curve was used as a measure of the MT firmness.

2.4. UVE

The UVE algorithm is used for variable selection based on analysis of the regression coefficients of PLS. This algorithm offers several advantages, such as simple procedure, faster execution, convenience, and accuracy, and has been widely used in chemical analysis fields in recent years. The algorithm's principle is as follows: an artificial random variable matrix $R(m \times n)$ with a very small amplitude is added to the original spectral matrix X, an $m \times n$ matrix containing n spectral responses of m samples. The regression coefficient matrix b is obtained using a leave-one-out cross validation (Centner et al., 1996), which represents the contribution of each variable to the established model. The reliability of each wavelength is analyzed by the following formula:

$$C_i = \frac{\text{mean}(b_i)}{s(b_i)}, \quad (2)$$

where mean(b) and s(b) are the mean value and standard deviation of the regression coefficients of the wavelengths, respectively. i denotes the i th wavelength. The larger the reliability C is, the more important the corresponding wavelength becomes. If a cutoff threshold is established, the variable with reliability below the threshold will be eliminated, and the remaining ones will be retained.

2.5. SAP clustering algorithm

SAP is a modification of the AP algorithm (Qian et al., 2009). In the spectral matrix X, each column is considered as a data point. The AP function is to find a data point k for each data point i as its exemplar. AP relies on the basis of a real-valued similarity collection $\{s(i,k)\}$ between data points, where each similarity $s(i,k)$ represents how well data point k is suited to be the exemplar for the data point i. In particular, $s(k,k)$ is defined as "preference" and suggests the priority suitability of wavelength k being an exemplar. It shows the number of wavelengths being selected as exemplars. Generally, low preferences leads to a small number of wavelengths, whereas high preferences leads to a large number.

Several measures can be used in constructing the similarity matrix, such as the Euclidean distance, the absolute distance, and so on, but the results obtained by these methods were poor. The Kullback–Leibler divergence Jan (2011) was used in the current paper. Accordingly, the divergence between wavelengths i and k is

$$KL(i,k)_{AP} = \sum_m X(m,i)\log\frac{X(m,i)}{X(m,k)} + \sum_m X(m,k)\log\frac{X(m,k)}{X(m,i)}. \quad (3)$$

As the divergence criterion is used as a measure of dissimilarity between two wavelengths, the similarity matrix can be calculated by

$$S(i,k)_{AP} = 1 - KL(i,k)_{AP}. \quad (4)$$

In this experiment, the actual firmness value of the sample can be used as the labeled information to adjust the similarity matrix. This is termed as SAP.

The present study adopted the absolute errors between the samples' actual firmness and predicted values for each wavelength to adjust the similarity matrix. The method is given by the following equation:

$$KL(i,k)_{SAP} = (1-k)\times\left\{\sum_m X(m,i)\log\frac{X(m,i)}{X(m,i)} + \sum_m X(m,k)\log\frac{X(m,k)}{X(m,i)}\right\} + k\times\left\{\sum_m \left|P(m,i)-Y(m,1)\right| + \sum_m \left|P(m,k)-Y(m,1)\right|\right\}, \quad (5)$$

where matrix $P_{m\times n}$ is the predicted firmness value of each sample with wavelengths from 500 to 1000 nm at 5 nm interval. $Y_{m\times 1}$ is the actual firmness value of each sample, and k is a weighing coefficient. The best prediction results in the current study are obtained when $k = 0.6$.

For $s(k,k)$, the preferences of all data points are generally set to the same value. Here, the "preference" of each wavelength can be estimated by kurtosis, a common measure of non-Gaussianity of a wavelength. The square of the kurtosis is used to compute the "preference" because the kurtosis may be negative. $s(k,k)$ is obtained by

$$s(k,k) = \alpha \times \left\{E(X_k^4) - 3\times\left\{[E(X_k^2)]^2\right\}\right\}^2, \quad (6)$$

where α is a common positive value for obtaining different number of exemplars and X_k represents the kth column of matrix X.

Table 1
Statistics of firmness measurements for apples.

	Mean (N)	Standard deviation (N)	Min (N)	Max (N)
All ($n = 600$)	56.65	12.07	31.22	88.50
Calibration set ($n = 450$)	55.55	12.54	31.22	88.50
Prediction set ($n = 150$)	59.95	9.85	37.64	77.03

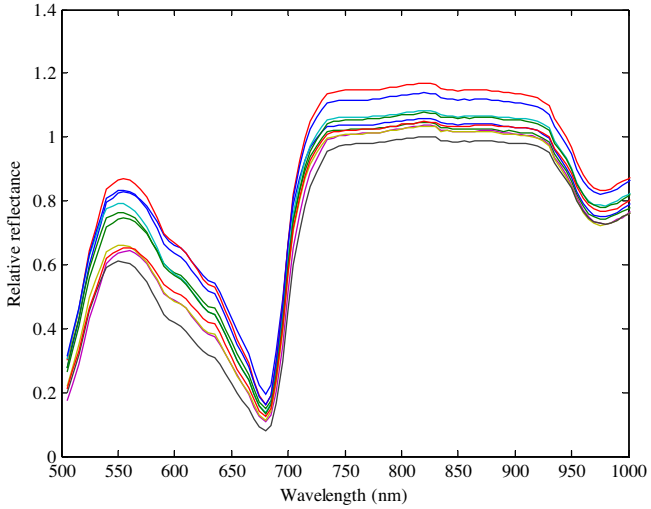

Fig. 3. Spectra of relative reflectance for 10 apples.

Table 2
Selected wavelengths by UVE and SAP algorithms (Unit: nm).

UVE (34)	Number	r_1	r_2	r_3	r_4	r_5	r_6	r_7	r_8	r_9	r_{10}
	Wavelength	525	530	600	605	630	635	640	650	655	660
	Number	r_{11}	r_{12}	r_{13}	r_{14}	r_{15}	r_{16}	r_{17}	r_{18}	r_{19}	r_{20}
	Wavelength	690	695	710	735	755	765	800	805	810	830
	Number	r_{21}	r_{22}	r_{23}	r_{24}	r_{25}	r_{26}	r_{27}	r_{28}	r_{29}	r_{30}
	Wavelength	840	845	850	855	870	900	905	910	920	945
	Number	r_{31}	r_{32}	r_{33}	r_{34}						
	Wavelength	950	985	990	995						
SAP (35)	Number	k_1	k_2	k_3	k_4	k_5	k_6	k_7	k_8	k_9	k_{10}
	Wavelength	500	505	510	515	520	525	530	545	575	590
	Number	k_{11}	k_{12}	k_{13}	k_{14}	k_{15}	k_{16}	k_{17}	k_{18}	k_{19}	k_{20}
	Wavelength	610	625	635	645	650	665	670	675	685	700
	Number	k_{21}	k_{22}	k_{23}	k_{24}	k_{25}	k_{26}	k_{27}	k_{28}	k_{29}	k_{30}
	Wavelength	705	710	720	745	800	810	815	820	855	900
	Number	k_{31}	k_{32}	k_{33}	k_{34}	k_{35}					
	Wavelength	920	930	940	980	1000					

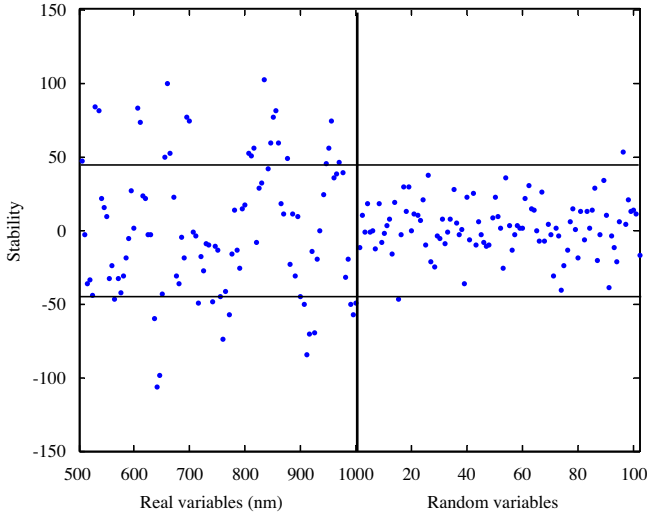

Fig. 4. Selecting wavelengths using the UVE algorithm.

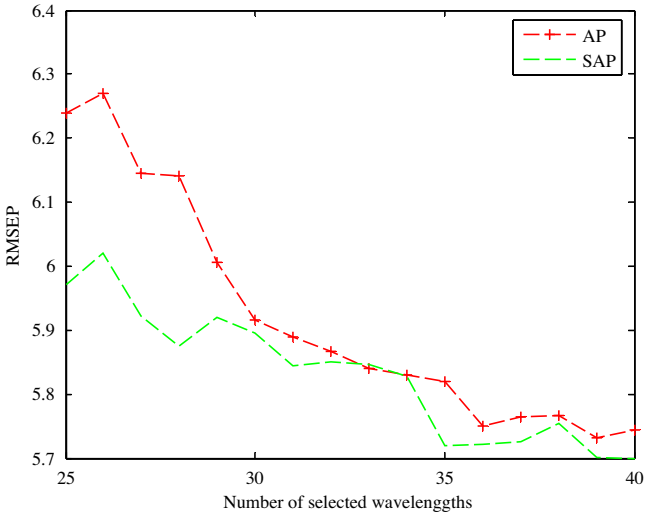

Fig. 5. RMSEP with the number of selected wavelengths by AP and SAP algorithms.

2.6. Model fusion using BP neural network

The apple samples were divided into two data sets (calibration and prediction sets) using the Kennard–Stone algorithm (Karolien et al., 2010), which used the Euclidian distances of the phase point in phase space to find the representative samples. For the calibration set, 450 apples were chosen, whereas the remaining apples were used for the prediction set. The statistics are shown in Table 1.

In general, a prediction model built by a single algorithm lacks generalization ability. The reliability of the model is also unstable due to measurement noise. The data fusion method, however, considers the relationship among different data sources and has significant advantages over single source data. Thus, using data fusion method improves the generalization ability and the stability of the model. The UVE algorithm can improve the prediction ability of the PLS model because it takes into account the combination of spectral response information with the labeled information (actual firmness). However, extra random variables make the algorithm unstable during the wavelength selection. The SAP algorithm is an efficient and fast clustering algorithm, but it lacks supervision over the effective labeled information, which focuses on analyzing the similarity among wavelengths. This complementary information between the two algorithms must be utilized to improve the

Table 3
Results of models by different wavelength selection algorithms.

Method	Number*	Factors	Rc**	RMSEC** (*N*)	Rcv**	RMSECV** (*N*)	*Rp***	RMSEP** (*N*)
Full	101	10	0.873	6.05	0.852	6.46	0.791	6.00
UVE	34	9	0.874	6.08	0.858	6.43	0.805	5.85
AP	39	11	0.865	6.29	0.849	6.63	0.813	5.73
SAP	35	11	0.865	6.29	0.849	6.62	0.814	5.71
UVE–SAP	27	10	0.870	6.19	0.857	6.46	0.808	5.80
SAP–UVE	10	8	0.815	7.26	0.805	7.43	0.795	6.03
Fusion model	–	–	0.885	5.95	–	–	0.828	5.53

* Number of selected wavelengths by different methods.
** Rc = coefficients of correlation between the predicted values and the actual value, RMSEC = root mean square error for calibration, Rcv = cross-validation correlation coefficient. RMSECV = root mean square error for cross-validation. *Rp* = coefficients of correlation for prediction. RMSEP = root mean square error for prediction.

performance of a single algorithm. The data fusion technology combines the advantages of each algorithm and minimizes the weaknesses of the different algorithms. At present, the BP neural network is universally used in data fusion technology. The BP neural network has a strong fault tolerance, is self-learning and self-organizing, and has adaptive ability, which can simulate complex nonlinear mapping. It can also process incomplete, imprecise, and even fuzzy data. These characteristics of the BP neural network and the strong nonlinear approximation capacity completely meet the requirements of data fusion technology. In summary, if these two algorithms were fused by BP, the limitations of the two algorithms can be overcome, and the prediction ability of the model will significantly improve.

There are three levels of fusion according to the data fusion theory (Varshney, 1997), namely, data, feature, and decision fusions. Among these, the decision fusion level was chosen because it was a feasible approach. The BP neural network, composed of one input layer, one hidden layer, and one output layer, was adopted for the decision fusion level. The input and output layers are associated with the hidden layer through connection weights. For the present analysis, there were two nodes in the input layer and one node in the output layer. The UVE-PLS and SAP-PLS model prediction values of the calibration set were used for the input layer of the BP neural network. The output of the BP neural network model represented the final prediction values. The number of nodes for the hidden layer was optimized using the empirical formula

$$m = \sqrt{n+1} + \alpha, \tag{7}$$

where m, n, and l represent the number of nodes in the hidden, input, and output layers, respectively. The controlled parameter α ranges from 1 to 10. After simulation analysis by trial and error, the number of nodes for the hidden layer was set to five.

Five parameters were used to evaluate the performance of the calibration model. These include the coefficients of correlation for the calibration set (Rc), root mean-square error for the calibration set (RMSEC), cross-validation correlation coefficient (Rcv), root mean-square error for cross validation, and the number of principal factors. *R*p and RMSEP of the prediction set were two important parameters to evaluate the performance of the prediction model. Generally, a model with higher *R*p and smaller RMSEP is more satisfactory.

3. Results and discussion

3.1. Characterization of spectral scattering profiles

Fig. 3 shows the spectra of the relative reflectance of the 10 apples. The spectra emit two absorption downward peaks, one strong absorption peak at 675 nm and one weak absorption peak at 970 nm, due to chlorophyll and water absorption, respectively. The spectra are relatively smooth in the range of 730–920 nm.

3.2. Wavelengths selected by UVE

First, full wavelengths are used for the PLS model. Table 2 shows the performance parameters of the PLS model with full wavelengths. The performance of the model was poor because the hyperspectral scattering images contained many redundant data; wavelength selection was thus necessary to improve the accuracy of the prediction model.

The number of principal factors of PLS is an important parameter in the model, which can be obtained by cross validation of the

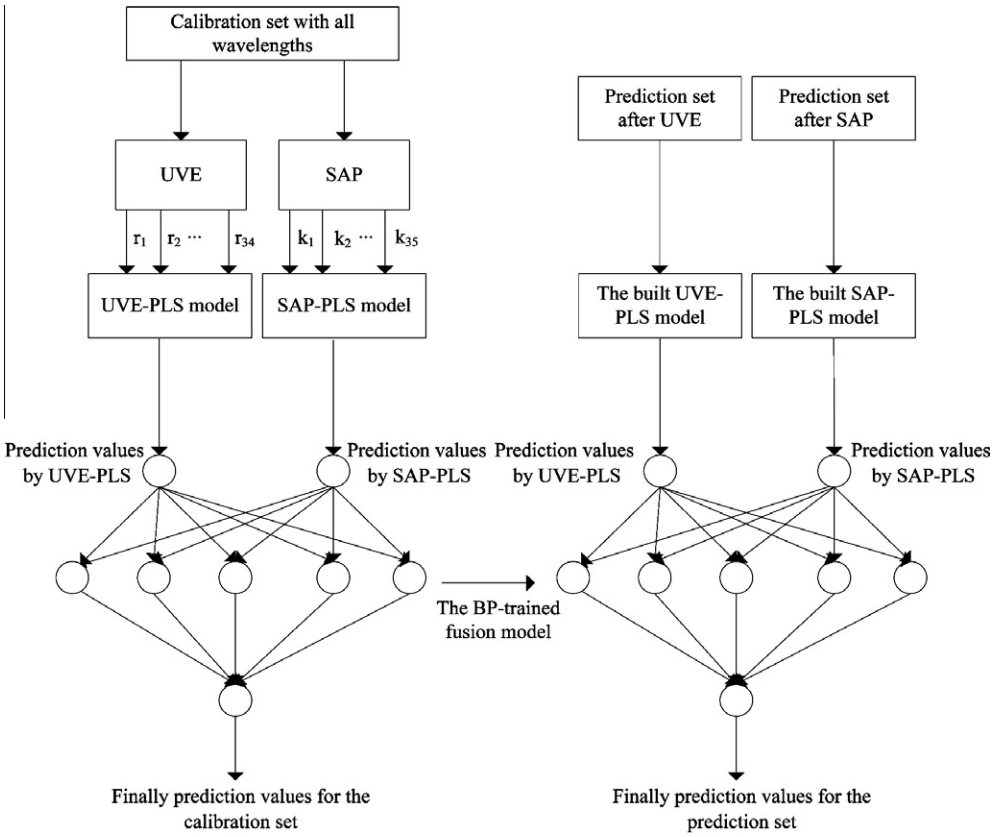

Fig. 6. Structure diagram of the BP fusion model.

calibration set. The number of factors for the UVE-PLS method was 9. Fig. 4 shows the stability of each wavelength in the range of 500–1000 nm for the calibration set using UVE. The two horizontal dotted lines represent the lower and upper thresholds. Based on the UVE principle, the wavelengths whose reliability lies within the dotted lines were eliminated, and the wavelengths whose stability lies outside the dotted lines were used for PLS calculation. After the application of the UVE algorithm, 34 wavelengths were selected, distributed mainly on two broad regions around 530–640 nm and 780–1000 nm. Table 2 shows the selected wavelengths. The information on the 34 wavelengths was used as the input of the PLS model, and the performances of the UVE-PLS model are shown in Table 3. The UVE-PLS model yielded better results than the PLS model with full wavelengths.

3.3. Wavelengths selected by AP and SAP

The main objective of the current study is to determine the number of selected wavelengths p, which relate to the stability and accuracy of the model. If the number of selected wavelengths is too small, the robustness and accuracy of the model might be affected because of the loss of informative wavelengths. On the contrary, if the number of selected wavelengths is too large, the complexity of the model will be increased. Therefore, the RMSEP parameter of the prediction set with the number of selected wavelengths p was investigated. Fig. 5 shows the varying tendencies of RMSEP for AP and SAP with selected wavelengths p from 25 to 40, respectively. The results obtained by the SAP method were better than those of AP. When p was 39, the lowest RMSEPs for SAP and AP were obtained, which were 5.70 and 5.73 N, respectively. However, for SAP, when p = 35 and 39, RMSEPs had the same value. The 35 wavelengths selected by SAP and the 39 wavelengths selected by AP were used for further analysis. Table 2 also shows the selected wavelengths by the SAP algorithm. The performances of the AP-PLS and SAP-PLS models are shown in Table 3. Compared with AP, SAP was more capable of optimizing the parameters of the PLS model. To obtain the minimum number of wavelengths with the most information, the current study also discussed UVE–SAP and SAP–UVE methods for selecting wavelengths. However, the PLS models did not achieve the desired results (Table 3) mainly because the two algorithms are based on different principles. To combine the advantages of the two algorithms, the present study thus developed the model fusion method.

3.4. Model fusion of UVE and SAP using BP neural network

To eliminate the limitations of using a single algorithm, a model fusion based on BP neural network is proposed in the current work. First, the fusion model of the BP neural network was established with the calibration set. The two nodes in the input layer of the BP neural network were the UVE-PLS and SAP-PLS model prediction values for the calibration set. The output layer of the BP neural network model was the final prediction values for the calibration set. The fusion model performance was then tested using the prediction set. Fig. 6 shows the structure diagram of the BP fusion model. The performance parameters of the fusion model of the BP neural network are shown in Table 3. The value of Rp increased by 4.6%, from 0.791 to 0.828. The RMSEP value decreased by 7.8%, from 6.00 to 5.53 N. These prediction results are better than the results (Rp by 1% and RMSEP by 3%) reported by Huang and Lu (2009). Figs. 7 and 8 show the data fusion model for predicting the firmness for the calibration set (Rc = 0.885 and RMSEC = 5.95 N) and for the prediction set (Rp = 0.828 and RMSEP = 5.53 N), respectively. The fusion model is thus preferred for predicting the firmness of apples because it improves the prediction accuracy compared with a single model.

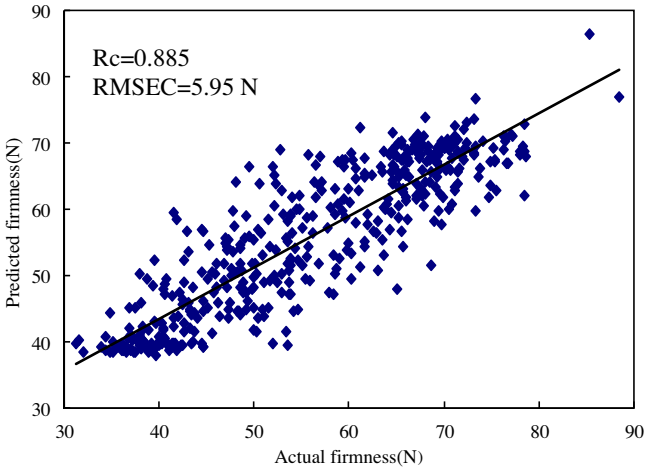

Fig. 7. Results of the fusion model between actual and predicted firmness for the calibration set.

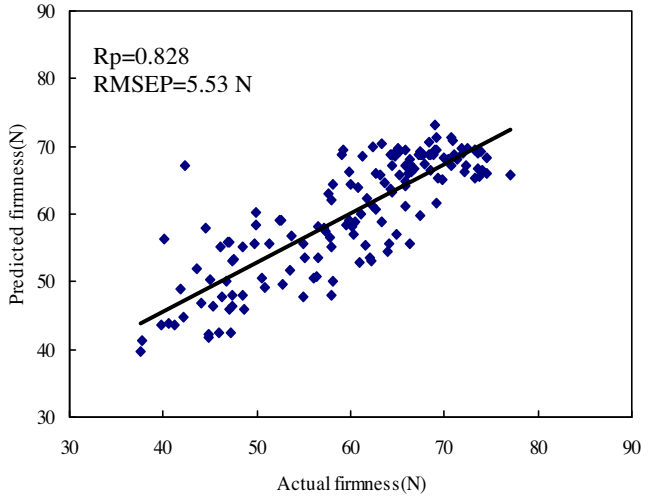

Fig. 8. Results of the fusion model between actual and predicted firmness for the prediction set.

4. Conclusion

The wavelength selection of hyperspectral scattering images based on UVE-PLS, SAP-PLS, and fusion models using the BP neural network was investigated in the current paper. Compared with using a single UVE-PLS or SAP-PLS model, the fusion model produced better prediction results for apple firmness, where the correlation coefficient increased to 0.828 and the RMSEP decreased to 5.53 N. The fusion model eliminated the limitation of the single algorithm and combined the advantages of the two algorithms. The fusion model is therefore an effective method for predicting apple firmness using hyperspectral scattering image.

Acknowledgments

Authors gratefully acknowledge the guidance of Dr. Lu who works at Postharvest Engineering Laboratory of US Department of Agriculture for this experiment and financial support from the National Natural Science Foundation of China (Grant No. 60805014), the Natural Science Foundation of Jiangsu Province (China, BK2011148) and the Fundamental Research Funds for the Central Universities (Grant Nos. JUSRP20913 and JUSRP21132).

References

Armstrong, P.R., Stone, M.L., Brusewitz, G.H., 1997. Peach firmness determination using two different nondestructive vibrational sensing instruments. Trans. ASAE 40, 699–703.

Centner, V., 2009. Multivariate Approaches: UVE-PLS. Chemical and Biochemical Data Analysis 21, 609–618.

Centner, V., Massart, D.L., De Noordb, O.E., 1996. Detection of inhomogeneities in sets of NIR spectra. Anal. Chim. Acta 330, 11–17.

Frey, B.J., Dueck, D., 2007. Clustering by passing messages between data points. Science 315, 972–976.

Huang, M., Lu, R., 2009. Optimal wavelengths selection using hierarchical evolutionary algorithm for prediction of firmness and soluble solids content in apples. ASABE Annual International Meeting 10, 6571–6582.

Jan, K., 2011. Combining marginal probability distributions via minimization of weighted sum of Kullback–Leibler divergences. Int. J. Approx. Reason 14, 1–13.

Karolien, S., Bernard, D.B., Ivan, S., Veerle, F., 2010. Subset selection from multi-experiment data sets with application to milk fatty acid profile. Compute. Electron. Agric. 73, 200–212.

Koumonsis, K., Katsaras, C., 2006. A saw-tooth genetic algorithm combining the effects of variable and reinitialization to enhance performance. IEEE Trans on Evolutionary Computation 10, 19–28.

Lu, R., 2001. Predicting firmness and sugar content of sweet cherries using near-infrared diffuse reflectance spectroscopy. Trans. ASAE 44, 1265–1271.

Lu, R., 2007. Nondestructive measurement of firmness and soluble solids content for apple fruit using hyperspectral scattering images. Sensing Inst. Food Quality & Safety 1, 19–27.

Lu, R., Peng, Y., 2006. Hyperspectral scattering for assessing peach fruit firmness. Biosys. Eng. 93, 161–171.

Min, M., Lee, W.S., 2005. Determination of significant wavelengths and prediction of nitrogen content for citrus. Trans. ASAE 48, 455–461.

Nicolai, B.M., Beullens, K., Bobelyn, E., Peirs, A., Saeys, W., Theron, K.I., Lammertyn, J., 2007. Nondestructive measurement of fruit and vegetables quality by means of NIR spectroscopy: a review. Postharv. Bio. Techn. 46, 99–118.

Peng, Y., Lu, R., 2006. An LCTF-based multispectral imaging system for estimation of apple fruit firmness. Part I. Acquisition and characterization of scattering images. Trans. ASAE 49, 259–267.

Peng, Y., Lu, R., 2008. Analysis of spatially resolved hyperspectral scattering images for assessing apple fruit firmness and soluble solids content. Postharvest Biol. Technol. 48, 52–62.

Qian, Y., Yao, F., Jia, S., 2009. Band selection for hyperspectral imagery using affinity propagation. IET comput. Vis. 34, 213–222.

Qin, J., Lu, R., 2007. Measurement of the absorption and scattering properties of turbid liquid foods using hyperspectral imaging. Appl. Spectrosc. 61, 388–396.

Qin, J., Lu, R., 2008. Measurement of the optical properties of fruits and vegetables using spatially resolved hyperspectral diffuse reflectance imaging technique. Postharvest Biol. Technol. 49, 355–365.

Varshney, P.K., 1997. Multisensor data fusion. Electronics & Communication Engineering Journal 9, 245–253.

Wu, D., He, Y., Feng, S., 2008. Shortwave near-infrared spectroscopy analysis of major compounds in milk powder and wavelength assignment. Ana1. Chim. Acta 610, 232–242.

Zude, M., Herold, B.J., Roger, M., Bellon-Maurel, V., Landahl, S., 2006. Non-destructive tests on the prediction of apple fruit flesh firmness and soluble solids content on tree and in shelf life. J. Food Eng. 77, 254–260.